Electronic structure of the Si-rich 3*C*-SiC(001)3×2 surface

H. W. Yeom*
Department of Physics and Measurement Technology, Linköping University, S-581 83 Linköping, Sweden and Research Center for Spectrochemistry, The University of Tokyo, Tokyo 113, Japan

Y.-C. Chao
Department of Physics and Measurement Technology, Linköping University, S-581 83 Linköping, Sweden

I. Matsuda
Department of Chemistry, The University of Tokyo, Tokyo 113, Japan

S. Hara and S. Yoshida
Electrotechnical Laboratory, Tsukuba, Ibaraki 305, Japan

R. I. G. Uhrberg
Department of Physics and Measurement Technology, Linköping University, S-581 83 Linköping, Sweden
(Received 7 April 1998)

The electronic structure of the Si-rich 3C-SiC(001) surface with a single-domain 3×2 long-range order has been studied by angle-resolved photoemission using synchrotron radiation. By identifying the topmost bulk valence band the Fermi level position at the surface is accurately determined to be located at 2.1 eV above the valence-band maximum. Four different surface state bands are clearly identified within the bulk band gap at 1.4±0.1, 2.3±0.1, 2.9±0.1, and 3.8±0.1 eV below the Fermi level, respectively. These states show no dispersion with photon energy in normal emission and both hydrogen adsorption and Si sublimation make them disappear. Dispersions and symmetry properties of the surface states were determined in detail. All four surface state bands have unusually small dispersions throughout the surface Brillouin zone suggesting strong localization of the electron orbitals within a unit cell and a unique surface bond configuration. The origins of the surface states observed in this study are ascribed to the dangling bonds of both the Si ad-dimers and the second layer Si atoms in the 3×2 surface reconstruction. [S0163-1829(98)04136-8]

I. INTRODUCTION

SiC is one of the most interesting noble device materials, especially for applications in various extreme environments involving high power, high temperature, and high frequency.[1–3] Since most of SiC material useful for device applications is fabricated by the chemical vapor deposition (CVD) technique, the microscopic surface structure information is of crucial importance for the control of the SiC thin film growth.[1–3] Along with its technological importance, SiC has attracted much recent attention in the surface science community due to its unique surface properties. SiC, which is not a covalent semiconductor in the ideal sense, has instead Si and C surface atoms in a ''polar'' environment. Thus it is of fundamental interest to study the reconstructions and electronic structures of Si and C atoms on such polar surfaces.

Among the numerous polytypes of SiC, most of the current discussion on surface properties has been devoted to cubic 3*C*-SiC(001) (Ref. 2) and hexagonal 6H(4H)-SiC(111) (Ref. 3) surfaces grown heteroepitaxially. It has been known that a well prepared 3C-SiC(001) surface exhibits three major surface phases according to its stoichiometry. That is, the carbon-terminated surface shows a $c(2\times2)$ reconstruction,[4–6] the Si-terminated surface a 2×1 [or $c(4\times2)$] (Refs. 5–9), and the Si-rich surface a 3×2 reconstruction.[10–14] The 3×2 surface consists of an additional Si layer on top of the Si-termination layer.[10–14] Although there is a wide consensus on the stoichiometry of these surface phases, the corresponding surface structures are under debate with contradicting structure models.[2,4–14]

Besides the geometrical structures of the surface reconstructions, there are interesting current issues on other surface properties of the 3C-SiC(001) surfaces. For example, the possibility of a unique sp^2 carbon dimer configuration was discussed for the carbon-terminated $c(2\times2)$ phase.[4] The Si-terminated surface exhibits a $c(4\times2)$-2×1 surface phase transition, which was suggested to be a metal-insulator transition.[9] In the case of the Si-rich surface, the issue of self-limiting Si layer growth[11,12] is still under debate and very interesting low dimensional structures of the zero-dimensional fluctuation (or a cellular disorder) (Ref. 15) and the highly stable one-dimensional chains[13] were observed.

In spite of such interesting ongoing discussions on the structural properties of the 3C-SiC(001) surfaces, only very few reports are available on the surface electronic structure, especially when it comes to experimental work. Most of the previous valence band photoemission studies of the 3C-SiC(001) surfaces have been done in the angle-integrated mode using soft x-ray synchrotron radiation.[16–20] Among them, only two groups have explicitly discussed surface features near the valence-band maximum (VBM) for the Si-

 © 1998 The American Physical Society

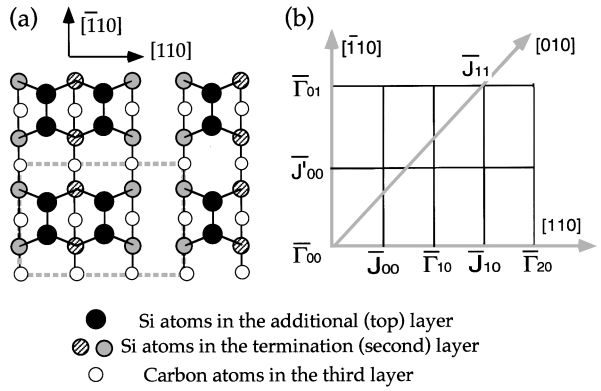

FIG. 1. (a) Schematic illustration of the 3C-SiC(001)3×2 surface structure with 2/3 ML of Si ad-dimers (the so-called Dayan-Hara model) (Refs. 10, 11, and 14). The surface unit cell is depicted by dashed lines and the surface Si atoms with different local registries are indicated with different symbols. (b) The corresponding 3×2 surface Brillouin zones drawn in a periodic zone scheme.

terminated 2×1 (Ref. 18) and the Si-rich 3×2 phases.[19] A similar surface feature was also observed recently for the Si-terminated $c(4\times2)$ surface.[9] No clear surface states have been identified for the carbon-terminated $c(2\times2)$ surface by valence-band photoemission. Very recently an experimental study of a double-domain 2×1 surface was reported, which identified two surface state bands within the bulk band gap.[21] By comparing with their own theoretical calculation the authors discussed the origin of the surface states as due to π and π^* states localized on the anomalous *weakly dimerized* Si surface atoms. However, detailed characterizations of the surface states, if existing, for the 3×2, $c(4\times2)$, and $c(2\times2)$ surfaces are still lacking and more detailed experimental studies were requested even for the 2×1 surface.[21] This situation prevents a proper understanding of the surface bond configurations and the mechanisms of the surface reconstructions for these important surfaces.

In the present paper, we report on an extensive angle-resolved photoemission study of a well-characterized single-domain 3C-SiC(001)3×2 surface using linearly polarized synchrotron radiation. For this surface we recently clarified the geometrical structure of its 3×2 reconstruction through high-resolution core-level photoelectron spectroscopy [see Fig. 1(a) and Ref. 14]. Four different surface state bands are clearly identified within the bulk band gap in the present study. The dispersions and symmetry properties of these surface state bands are determined in detail throughout the 3×2 surface Brillouin zone (SBZ). The characteristics and origins of these surface states are discussed in terms of the 3×2 surface reconstruction and the surface electronic structure information available in the literature.

II. EXPERIMENTAL DETAILS

Angle-resolved photoelectron spectroscopy (ARPES) measurements were performed on the new high-resolution spherical grating beam line (BL-33) at the Max-I synchrotron radiation facility in Lund, Sweden.[22] The beam line is equipped with an angle-resolved photoelectron spectrometer,[23] whose base pressure is $\sim 7.0\times10^{-11}$ mbar. The photoelectron energy analyzer is a 75-mm-radius hemispherical analyzer (ARUPS-10, VG Microtech) with a sophisticated electron lens whose acceptance angle can be varied electronically. The angular acceptance was set to the largest value (±2°) in order to maximize the count rate. The total energy resolution was set to ~150 meV at the photon energies ($h\nu$) used in this experiment (14–40 and 130 eV). Angle-integrated valence-band photoemission spectra were also taken at a photon energy of 130 eV,[14] for reference purpose, on the plane grating beam line (BL-22) of Max-I, which is equipped with a large hemispherical electron analyzer.

A well-ordered single-domain 3C-SiC(001)3×2 surface was prepared by annealing a CVD grown 3C-SiC(001) thin film at ~1180 °C in ultrahigh vacuum as described before.[11,14] The sample was heated very stably by direct resistive heating. A very sharp single-domain 3×2 low-energy-electron diffraction (LEED) pattern was observed with almost no noticeable minor domain (2×3) LEED spots. The streaks that are typically observed along the ×3 direction[2] were very weak at all primary electron energies. This high-quality LEED pattern together with the absence of any trace of oxygen in the photoelectron spectra indicate a high quality of the 3×2 surface phase prepared in this way. During the measurements repeated annealings at ~900 °C were done to get rid of possible residual gas contamination. These annealings did not affect the surface order or the stoichiometry.

In order to further confirm the surface state assignments, the 3×2 surface was exposed to atomic hydrogen at room temperature by facing the sample toward a hot tungsten filament in a hydrogen atmosphere. In this way, a very clear single-domain 3×1 LEED pattern was obtained as reported before.[2,11] A detailed characterization of the hydrogen-induced 3×1 phase by photoemission and LEED will be described elsewhere.[24]

ARPES spectra were measured along various axes of the 3×2 SBZ [see Fig. 1(b)], like $\bar{\Gamma}_{00}-\bar{J}_{00}$ (along the [110] azimuth), $\bar{\Gamma}_{00}-\bar{J'}_{00}$ (along [110]), and $\bar{\Gamma}_{00}-\bar{J}_{11}$ (along [010]). The [110] azimuth corresponds to the ×3 direction and is perpendicular to the Si ad-dimers as shown in Fig. 1(a). The steps in the polar emission angle (θ_e) were chosen to be 3° for each series of spectra for a given azimuth. The Fermi level position was determined from a well cleaned Ta surface in good electric contact with the sample.

Two different measurement geometries (called A_+ and $A_\pm$) were used to determine the symmetries of the surface-state wave functions with respect to the two mirror planes, which contain the [110] and [$\bar{1}$10] axes.[25] In the A_+ geometry photoelectrons are collected in the plane defined by the surface normal and the direction of the incident light. Since the *A* vector of the incoming, linearly polarized, synchrotron radiation lies in the plane of emission, in the A_+ geometry, only electronic states with even initial-state symmetry with respect to the mirror plane are observed. On the other hand, for the $A_\pm$ geometry the emission plane is kept perpendicular to the plane mentioned above. In this case the *A* vector has both parallel and perpendicular components to the emission plane. Therefore, both even- and odd-symmetry states are excited in this geometry. Through comparison of the spectra for a mirror plane obtained with these two different geom-

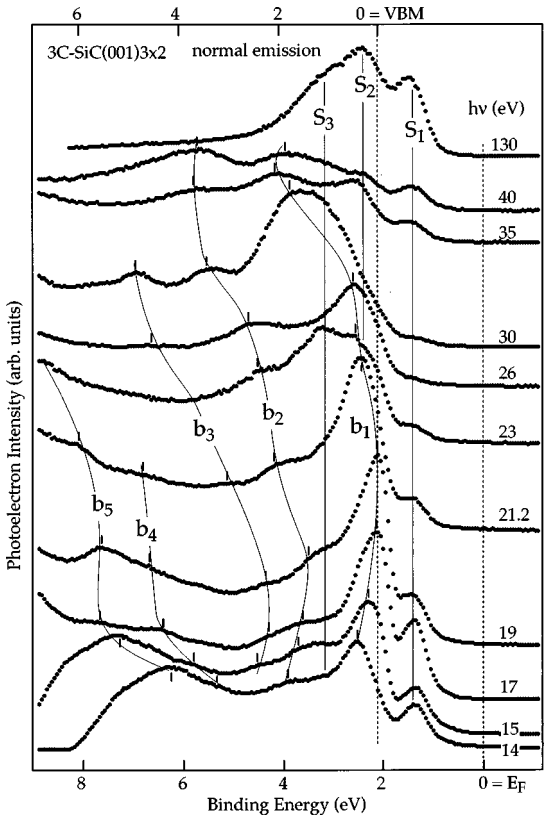

FIG. 2. ARPES spectra for the single-domain 3C-SiC(001)3 $\times 2$ surface taken at normal emission for different photon energies. Thin solid lines connect features of similar origins. The position of bulk valence-band maximum (VBM) as determined from the spectra is indicated (see text). The binding energies are indicated with respect both to the Fermi level and to the VBM.

etries, the symmetry of a surface state (even or odd) can be determined. The ARPES spectra shown below are taken in the A_+ geometry if not specified differently.

III. ARPES RESULTS

A. Normal emission spectra and the valence-band maximum

A series of valence-band photoemission spectra for the 3×2 surface taken at normal emission ($\theta_e = 0°$) with different photon energies are shown in Fig. 2. Five different dispersing spectral features, denoted $b_1 - b_5$, and three nondispersing ones, denoted $S_1 - S_3$, can be identified in the spectra. The structures $b_1 - b_5$ are identified as due to bulk transitions since they show dispersions with photon energy; i.e., their initial energy changes as a function of k_n (the wave vector component normal to the surface). Contrary to these bulk structures surface-related features should have no dispersion in normal emission, since k_n is not a good quantum number for the two-dimensional electronic states localized on the surface layers. Thus the structures $S_1 - S_3$ are surface-state candidates since they have a constant binding energy irrespective of the photon energy. The four dispersing bands $b_2 - b_5$ and one nondispersing band S_1 with the lowest binding energy do not overlap one another, which makes them easy to identify. The structure b_1 interferes with S_2 and S_3 at $h\nu < 26$ eV, which makes the identifications more difficult. This problem is addressed below.

Based on their constant binding energies as a function of photon energy and their sensitivity to hydrogen adsorption, as discussed in detail below, we interpret structures $S_1 - S_3$ as surface-related features. The spectrum taken at $h\nu = 130$ eV in Fig. 2 can be compared to the previous angle-integrated study of Bermudez and Long performed at the same photon energy.[19] From the binding energy, S_1 can be easily identified to correspond to the topmost valence state of this previous study (denoted V_1 in Ref. 19 following Shek *et al.*[18]), which was suggested as a surface state of the 3 $\times 2$ surface. In this comparison, it is also worthwhile to note that no trace of oxygen $2p$ levels, at binding energies of 7–8 eV,[18,20] can be found in the present spectra for any of the photon energies.

By identifying S_1 and S_2 as surface-related features, the dispersing band b_1 is definitely the bulk feature with the lowest binding energy. Naturally this structure is interpreted as due to a direct transition from the uppermost valence band. Qualitatively, the dispersion of b_1 as a function of k_n is what one can expect from the theoretical calculation of the bulk 3C-SiC band structure.[26] Then by measuring the lowest binding energy of b_1, we can accurately determine the position of the VBM at Γ to be 2.1 eV below the surface Fermi level position as indicated in Fig. 2. Bermudez and Long[19] have estimated the VBM of the carbon-terminated 3C-SiC(001)$c(2\times 2)$ surface to be located at $\sim$2.0 eV below the Fermi level and they implied a similar value for the 3×2 and 2×1 phases. A very recent ARPES study of the 2×1 surface gave an estimated value of 1.7 eV below the Fermi level for the VBM position.[21] It should be noted that the extrapolation as used in these previous studies is not a quantitatively accurate way of determining the VBM position. Nevertheless, the VBM position determined in the present study qualitatively agrees with the previous estimates although the VBM position can depend on the sample preparation and doping levels. In fact, the surface Fermi level position was found to vary from the 3×2 to the carbon-terminated $c(2\times 2)$ surface[27] as well as to the 3×1 phase formed by hydrogen adsorption by roughly 0.2 eV (see below and Ref. 24). This indicates that there is a surface band bending at least larger than 0.2 eV for the 3×2 surface and that the bulk Fermi level of this SiC film is located at 1.9 eV above the VBM or lower. The band gap of SiC is known to be 2.4 eV, which implies that the bulk Fermi level is located close to the conduction-band minimum. This is what one can expect from the *n*-type doping: the CVD grown SiC films as used in the present study are unintentionally doped by nitrogen impurities.[28]

The position of the VBM in turn confirms the surface nature of the topmost valence-band feature S_1, since this state is well inside the fundamental bulk band gap. The second surface feature S_2 is located just below the VBM and it interferes with b_1 for most photon energies in Fig. 2. The S_3 state at a binding energy of 2.9 eV as well as S_2 will be discussed as a surface state in detail below.

B. Detailed ARPES measurements and surface state bands

Figures 3 and 4 show the detailed ARPES spectra taken at 21.2 and 17.0 eV, respectively, for the 3C-SiC(001)3×2 surface along the [110] azimuth, which corresponds to the

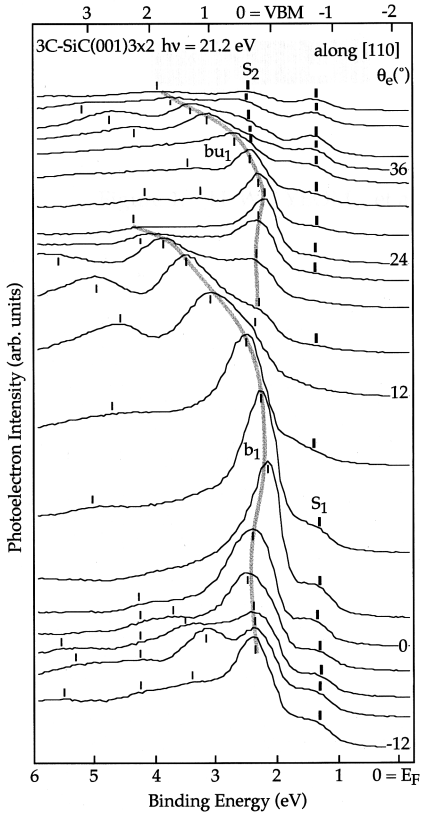

FIG. 3. ARPES spectra from the single-domain 3C-SiC(001)3 $\times 2$ surface taken with linearly polarized synchrotron radiation ($h\nu = 21.2$ eV) along [110] ($\bar{\Gamma}_{00}-\bar{J}_{00}-\bar{\Gamma}_{10}-\bar{J}_{10}-\bar{\Gamma}_{20}$). The step in emission angles (θ_e's) is 3°. The photon incidence angle with respect to the surface normal is 45°. Each spectrum is normalized to the intensity above the Fermi level, which is proportional to the incident photon flux. The binding energies are indicated with respect both to the Fermi level and to the VBM. The peak positions of surface states and the bulk features are indicated with thick and thin tick marks, respectively. The thick gray lines trace the dispersions of the bulk band b_1 and its surface Umklapp counterpart bu_1 (see text).

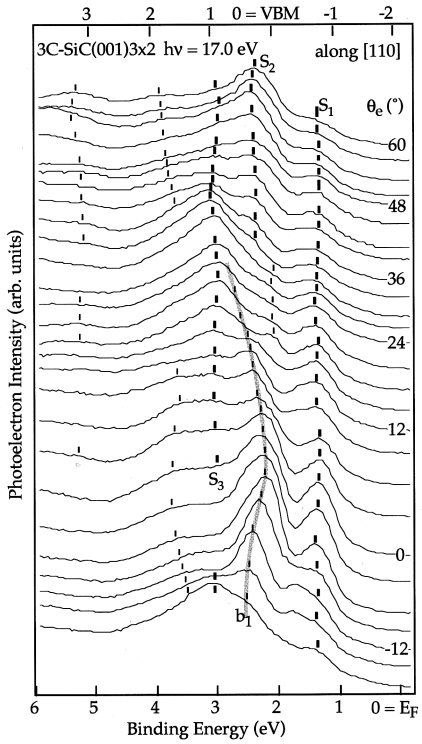

FIG. 4. Same as Fig. 3 except for the photon energy ($h\nu = 17.0$ eV).

$\times 3$ direction [see Fig. 1(a)]. In Fig. 3, the most dominant feature is the dispersing band b_1 mentioned above for the normal emission spectra. This band disperses steeply to higher binding energies for the emission angles larger than 10° with a decreasing intensity until it fades away at $\theta_e \sim 24°$. At lower binding energies, the surface state S_1 mentioned above is observed at most emission angles. S_1 shows almost no noticeable dispersion as function of emission angle.

Besides these two prominent bands, there is another characteristic band, denoted bu_1 in Fig. 3, at $\theta_e > 12°$ with binding energies of 2–4 eV. Although the intensity of bu_1 is much weaker than b_1, the dispersion and intensity variation of bu_1 resemble those of b_1 very much. If we plot the dispersion curves of these bands with respect to the parallel component of the electron wave vectors k_p as in Fig. 5 (see the closed circles), it can be easily seen that bu_1 disperses in exactly the same way as b_1 except for an overall shift in k_p. As evident in the figure, this shift in k_p corresponds well with the size of an irreducible 3×2 SBZ ($\bar{\Gamma}_{00}-\bar{\Gamma}_{10}$). This unambiguously indicates that bu_1 is due to a surface Umklapp process of the b_1 band. The fact that the intensity variation of bu_1 mimics that of b_1 except for an overall reduction supports the interpretation that bu_1 and b_1 originate from the same initial state. Although it has been very rare to identify a Umklapp state for clean or adsorbed Si surfaces,[29] it has been well known that a few compound semiconductor

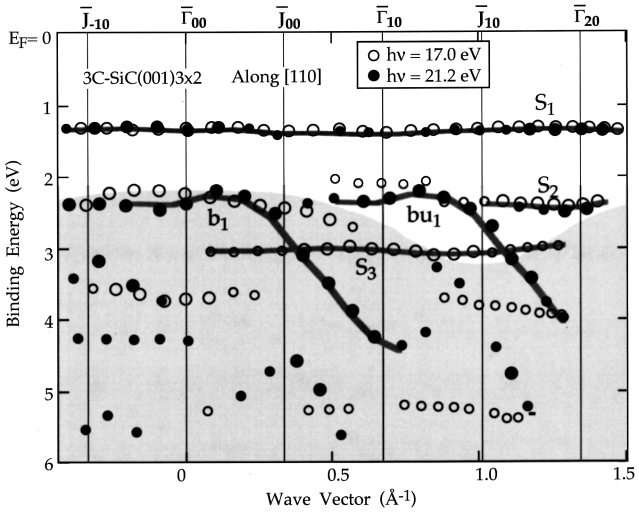

FIG. 5. Experimental dispersions for the single-domain 3C-SiC(001)3$\times$2 surface along the [110] azimuth derived from the spectra shown in Figs. 3 (solid symbols) and 4 (open symbols). The small and the large symbols correspond to relatively distinctive and weak spectral features, respectively. The hatched area is the bulk valence band projected onto the 1×1 surface Brillouin zone. The dispersions determined for the surface states and major bulk-related bands are depicted by gray lines.

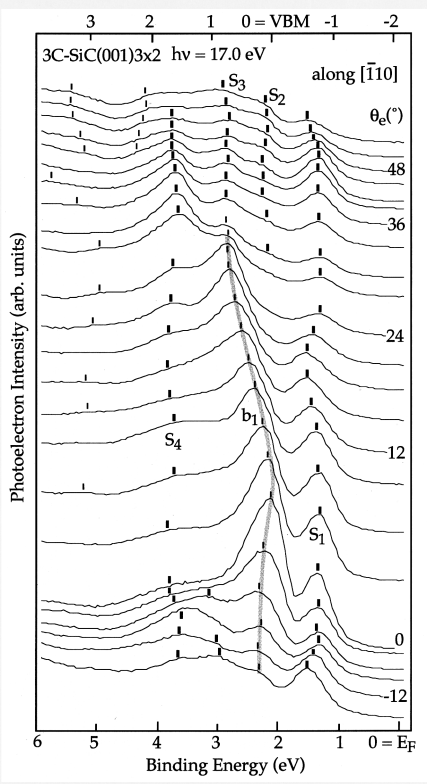

FIG. 6. Same as Fig. 4 except that the azimuth is the $[\bar{1}10]$ direction ($\bar{\Gamma}_{00}-\bar{J'}_{00}-\bar{\Gamma}_{01}$).

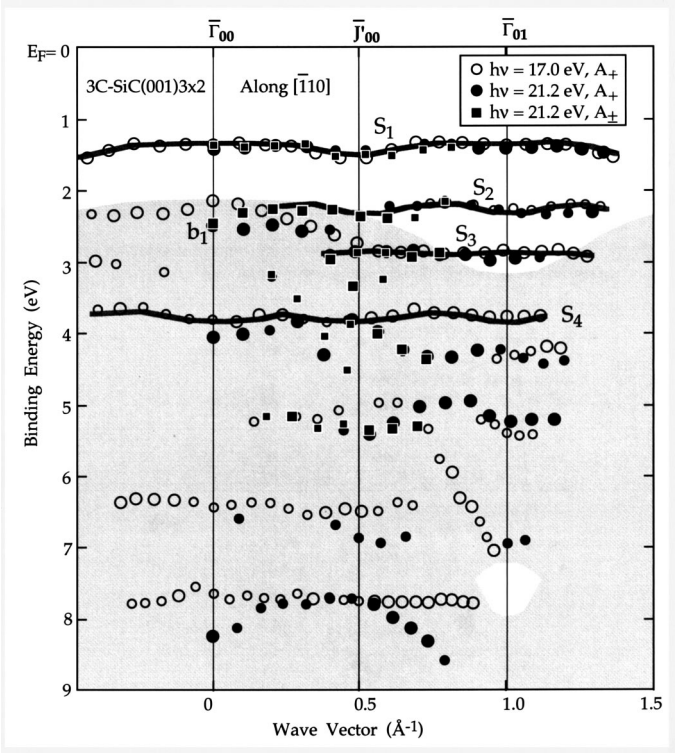

FIG. 7. Dispersions along the $[\bar{1}10]$ azimuth derived from the spectra shown in Fig. 6 (open circles) and from the spectra obtained at $h\nu=21.2$ eV using both the A_+ (closed circles) and $A_\pm$ (closed squares) geometries (the spectra not shown here).

surfaces show distinctive surface Umklapp transitions of the topmost bulk bands in ARPES spectra.[30]

A rather weak but discernible state can also be identified at a binding energy of ~2.4 eV for $\theta_e>36°$. Since this band is above the uppermost bulk band b_1 or its Umklapp branch bu_1, this state must be a surface state. From its binding energy and flat dispersion in k_p as shown clearly below, this state is identified as the S_2 state observed in normal emission for photon energies higher than 30 eV (see Fig. 2). There are also several other features with binding energies higher than ~3 eV, which will not be discussed here.

In similar ARPES scans obtained with $h\nu=17.0$ eV (see Fig. 4), the b_1 band also dominates around normal emission. The dispersion of b_1 is different from that observed at $h\nu=21.2$ eV, showing smaller downward dispersion up to a binding energy of ~3 eV. At this photon energy, S_1 is rather intense, which makes its minimal dispersion in k_p very obvious. At high emission angles, S_2 appears at the same energy as in the spectra for $h\nu=21.2$ eV but with much higher intensity. In addition to the states mentioned above, another weakly dispersing band is observed at ~3.0 eV for most emission angles. From the binding energy we identify this state with S_3 mentioned in Fig. 2.

The detailed dispersion curves of the valence-band features along the [110] azimuth, measured with two different photon energies, are shown in Fig. 5. It is very clear that the dispersions of the S_1 and S_2 states are the same for the two photon energies, which should be the case for a surface state. The surface nature of S_1 and S_2 is also verified by their energy positions, which are well within the bulk band gap. S_2 has a binding energy similar to b_1, but it cannot be assigned to yet another surface Umklapp of b_1 for the following reasons. (1) At $h\nu=17.0$ eV, S_2 appears with a strong intensity only around $\bar{\Gamma}_{20}$ but is not observed around $\bar{\Gamma}_{10}$ and (2) the intensity variation of S_2 from J to $\bar{\Gamma}$ is definitely different from that of b_1. The third flat band S_3 observed for $h\nu=17.0$ eV is partly located within the bulk band gap suggesting that it is a surface state. The photon energy independence of the dispersion of S_3 is not certain along this azimuth, but it will be verified along the [110] azimuth below.

Figure 6 shows the ARPES data obtained with $h\nu=17.0$ eV in the mirror plane of the 3×2 surface containing the [110] azimuth. The corresponding dispersion curves are shown in Fig. 7 together with the data taken at $h\nu=21.2$ eV. For the ARPES scan at $h\nu=21.2$ eV, the dispersion data taken with both the A_+ and $A_\pm$ geometries are included in the figure. Closed circles and closed squares are used for the A_+ and $A_\pm$ geometries, respectively. As shown in Fig. 6, the topmost bulk band b_1 has a similar dispersion to that along the [110] azimuth. However, no distinctive surface Umklapp band is observed in contrast to the [110] azimuth. Although it is not so easy to distinguish the S_3 band from b_1 in this figure, we can assign the surface-state band S_3 from the corresponding ARPES spectra taken at 21.2 eV not shown here. As shown in Fig. 7, the S_3 band lies within the band gap near $\bar{\Gamma}_{01}$. The photon energy independence of S_3 within the band gap near $\bar{\Gamma}_{01}$ corroborates its surface nature. Along the [110] azimuth, S_1 shows a small but noticeable dispersion: it disperses to higher binding energy from $\bar{\Gamma}$ towards J. As apparent in Fig. 7, this dispersion definitely follows the periodicity of the SBZ ruling out the possibility of a defect origin for this surface state. While similar disper-

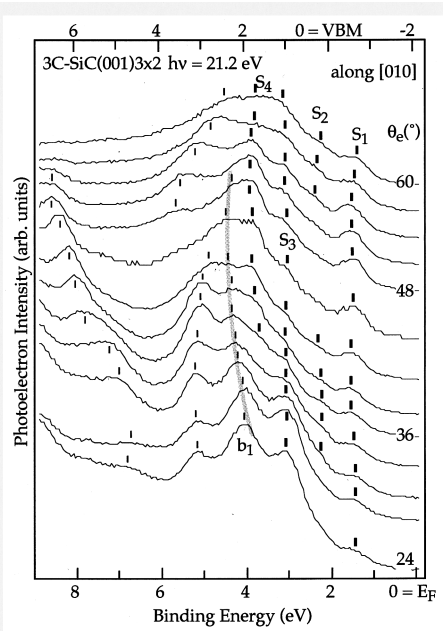

FIG. 8. ARPES spectra obtained at $h\upsilon = 21.2$ eV along the [010] azimuth ($\bar{\Gamma}_{00} - \bar{J}_{11}$).

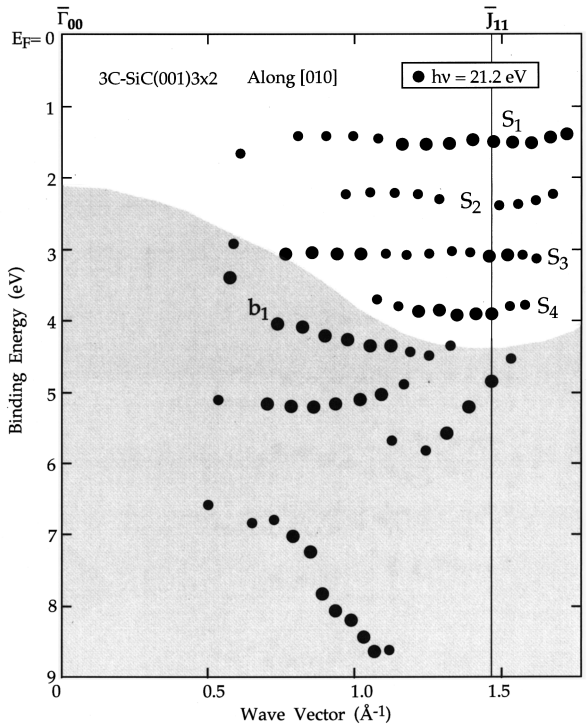

FIG. 9. Dispersions along the [010] azimuth derived from the spectra shown in Fig. 8.

sions are noticed for the second surface state S_2, no dispersion of S_3 could be detected. Along [110], we observe another band S_4 with a small dispersion at a binding energy of 3.8 eV. Although the dispersion of S_4 seems to follow the SBZ symmetry, its surface nature is not clear at this point. The surface state nature of S_4 will, however, be made unambiguous below.

Although we do not probe a mirror plane, the ARPES spectra along the diagonal axis [010] can be very helpful to identify a surface state since the projected bulk band gap extends down to a binding energy of 4 eV (~2 eV below the VBM). The ARPES data taken along [010] azimuth, especially around $\bar{J}_{11}$, where the bulk band gap is widest, are shown in Fig. 8. The corresponding dispersion curves are depicted in Fig. 9. In this figure, we observe all four bands $S_1 - S_4$, which are located clearly within the bulk band gap at the same binding energies as along the [110] and [110] azimuths. This unambiguously confirms the surface nature of these four flat bands.

C. Change in the surface state emission by Si sublimation and hydrogen adsorption

Up to now, we have shown that there are four surface state bands denoted $S_1 - S_4$ within the bulk band gap. One can further confirm the surface nature of these bands by checking their sensitivity to any modification of the surface structure/stoichiometry. Changes of the surface stoichiometry can be induced by sublimation of Si at ~1180 °C: annealing at this temperature leads to Si sublimation from the 3×2 surface and subsequently the surface evolves to the Si-terminated 2×1 phase and finally to the C-terminated $c(2\times2)$ phase.[2] Figure 10(a) shows the corresponding angle-integrated valence-band spectra taken at 130-eV photon energy for the three different surface phases obtained by such annealings. The surface quality of each phase has been checked by a previous high-resolution core-level photoemission study.[14,31] As is evident in Fig. 10(a), the S_1, S_2, and S_3 surface states have vanished for the 2×1 and $c(2\times2)$ phases. This fact clearly demonstrates that S_1, S_2, and S_3 are surface states intrinsic to the 3×2 phase. It can be noted that the spectra for the 2×1 and $c(2\times2)$ phases are qualitatively consistent to those previously reported by Bermudez and Long.[19] While the previous conclusion for the topmost state S_1 (denoted V_1 in the previous study) was in agreement with the present result, the S_2 and S_3 surface states have not been identified before.[19] Shek *et al.* have measured angle-integrated spectra of the 2×1 surface at a photon energy of 65 eV and assigned two features at binding energies of ~1.6 and ~2.6 eV, denoted V_1 and V_2, to surface states.[18] These two features showed a clear sensitivity to oxygen adsorption. This previous spectrum is very similar in shape and binding energies of the peaks to our spectrum taken at a photon energy of 40 eV in Fig. 2. From this similarity, one may relate the surface states S_1 and S_2 of the 3×2 surface to V_1 and V_2 of the 2×1 surface as was already implied by Bermudez.[2,19] This point will be discussed further below.

An way to alter the surface structure of the 3×2 surface is provided by the atomic hydrogen exposure. As reported previously,[2,11] a very clear single-domain 3×1 LEED pattern was obtained by atomic hydrogen exposure to the 3×2 surface at room temperature.[24] Although the detailed structure of the 3×1-H phase is to be investigated,[24] it is believed that hydrogen atoms are bonded to the Si surface atoms in such a way that the Si ad-dimers of the 3×2 phase are broken.[2] Extensive ARPES measurements were performed for the 3×1-H phase[24] and Fig. 10(b) compares typical ARPES spectra for the 3×2 (dots) and 3×1-H (solid lines) phases.

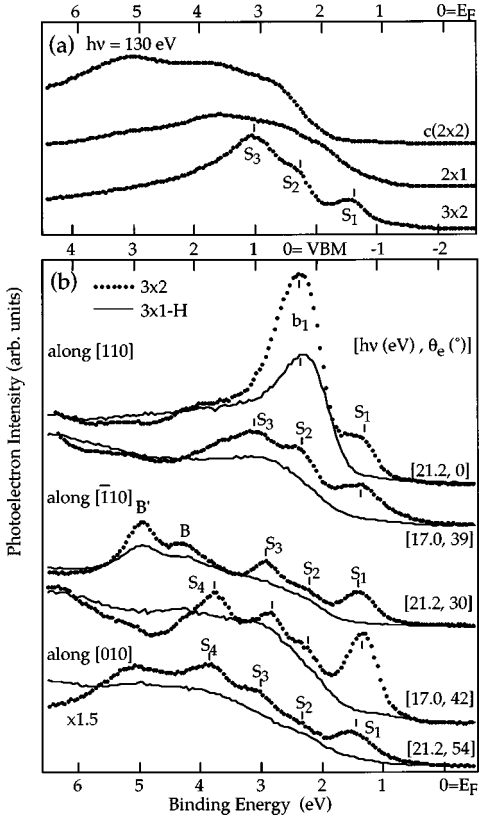

FIG. 10. (a) Comparison between the angle-integrated valence-band photoelectron spectra taken at $h\nu = 130$ eV for the 3C-SiC(001)3×2, 2×1, and $c(2\times2)$ surfaces obtained by annealing at ~1180 °C. (b) Comparison between the ARPES spectra for the 3C-SiC(001)3×2 (dots) and 3×1-H (solid lines) surfaces at five different emission angles (θ_e) along the three major azimuths ([110], [1̄10], and [010]). The major bulk and surface-state peaks are indicated. The binding energies are indicated with respect both to the Fermi level and to the VBM.

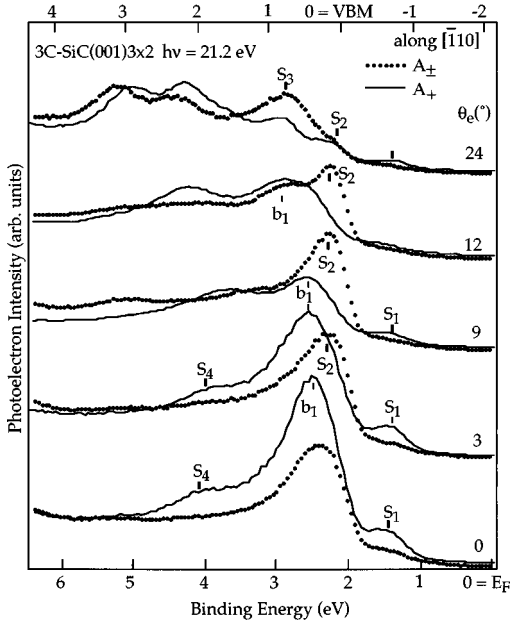

FIG. 11. Polarization-dependent ARPES spectra for a single-domain 3C-SiC(001)3×2 surface taken at $h\nu = 21.2$ eV along the [110] axis. Two different measurement geometries, even-symmetry sensitive A_+ (solid lines) and odd- and even-symmetry sensitive $A_\pm$ (dots) geometries were used to obtain the spectra. The corresponding emission angles (θ_e) are indicated. The photon incidence angle, with respect to the surface normal, is 45° and 15° for A_+ and $A_\pm$ geometries, respectively. All spectra are normalized to the background intensity above E_F. The binding energies are indicated with respect both to the Fermi level and to the VBM.

At first, by measuring the binding energy shift of the bulk related features [for example, b_1, B, and B' in Fig. 10(b)], the 3×1-H phase is found to have a 0.27 eV smaller band bending than the 3×2 phase.[24] This band-bending shift was corrected for when plotting the spectra shown in Fig. 10(b). The comparison of the spectra for the 3×1-H and 3×2 phases unambiguously shows that all surface state bands S_1-S_4 are quenched by the formation of the 3×1-H phase. This provides another very clear evidence that the four bands S_1-S_4 are intrinsic surface state bands of the 3×2 phase. Along with the change of the surface states, one can notice that the topmost bulk band b_1 shows an intensity decrease upon hydrogen exposure (see the normal emission spectra taken along [110]). Two possible reasons can be mentioned: (1) the predominant peak assigned as b_1 can have some contribution from the S_2 surface state having the same binding energy at $\bar{\Gamma}$ or (2) hydrogen adsorption may induce surface disorder to some extent, which can lead to diffuse scatterings of photoelectrons. Although the increase of surface disorder for the 3×1-H phase was not evident in its LEED pattern, we think that the latter possibility cannot be ruled out completely at this point.

D. Symmetry properties of the surface states

After having unambiguously identified the four surface state bands within the bulk band gap, we further investigated the symmetry properties of these surface states in the two mirror planes containing the [110] and [1̄10] azimuths. The surface state can have either even or odd symmetry with respect to the mirror planes, which can be determined by comparing ARPES data taken at two different geometries, $A_\pm$ and A_+, as explained above. Figure 11 shows a comparison of the ARPES spectra obtained for the $A_\pm$ (dots) and A_+ (lines) geometries along the [110] azimuth. While the S_1 and S_4 states appear with much smaller intensities in the $A_\pm$ geometry, the S_2 and S_3 states show a clear enhancement. This indicates that S_1 (S_4) and S_2 (S_3) have different mirror symmetries, even and odd, respectively. The enhancement of S_2 in the $A_\pm$ geometry is very drastic and makes it clear that S_2 overlaps with b_1 around normal emission as mentioned above for hydrogen adsorption. Similar polarization-dependent ARPES measurements were also done along the [110] azimuth and showed that S_1 (S_2) and S_3 have even and odd symmetries, respectively. The symmetry of S_4 was not certain since this state was not clearly observed along [110]. From this result, it is clear that the four surface states are *not symmetrically degenerate*.

IV. DISCUSSION

A. Overall characteristics of surface state dispersions and their implication

From the extensive ARPES measurements of a well ordered 3×2 phase, we identify four surface state bands

S_1-S_4 within the bulk band gap at 1.4 ± 0.1, 2.3 ± 0.1, 2.9 ± 0.1, and 3.8 ± 0.1 eV below the Fermi level, respectively. The most characteristic feature of these surface state bands is the fact that they all have very small dispersions throughout the 3×2 SBZ. The magnitude of the dispersions is ~0.2 eV at most and the only discernible dispersions are observed for S_1, S_2, and S_4 along the [110] azimuth. This is reasonable in the sense that the [110] azimuth corresponds to the $\times2$ direction, in which the repeat distance of the surface structure is shortest.

The surface states with very small dispersions that we present here are in sharp contrast to the surface states of Si dimers on the Si(001)2×1 [or $c(4\times2)$] surface, which have dispersions larger than ~0.8 eV: ~0.8 eV for the dangling-bond surface state and much larger dispersions for the back- and dimer-bond surface states.[32] Similar values of the dispersions were also observed for the surface states of Ge dimers on the clean Ge(001)2×1 (Ref. 33) and on the Si(001)2×1 surface.[34] In the cases of well-known compound semiconductor surfaces such as InAs(001)2×4 (Ref. 35) and GaAs(001)2×4,[36] the surface states within the band gap have noticeable dispersions larger than 0.4 eV. Since all of the surfaces mentioned above including 3C-SiC(001)3×2 are based on dimer reconstructions, the small dispersion of the SiC(001)3×2 surface is exceptional. This directly indicates that the orbitals for the surface states S_1-S_4 are well localized. Similar nondispersing surface states were recently observed for the InP(001)2×4 surface.[37] This result was then interpreted as evidence of well isolated surface unit cells due to the unique surface structure probably not based on dimers. However, since the surface structure is based on Si dimers in the case of the 3C-SiC(001)3×2 surface, the nondispersing surface states suggest a unique bond configuration of the surface Si dimers.

Very recently we observed a unique fluctuation termed ''cellular disorder'' among the unit cells of the SiC(001)3×2 surface in scanning tunneling microscopy (STM) images indicating an extremely small correlation between the surface unit cells.[15] This observation is consistent with the nondispersing properties of surface-state bands suggesting a minimal overlap of surface electron orbitals between the neighboring unit cells.

Another recent STM study reported that the dimer rows of the 3×2 surface form very long, highly stable, one-dimensional lines.[13] However, the present result of the dispersionless surface-state bands without significant anisotropy indicates no strong interaction even along the dimer row direction. This suggests that the stability of the long one-dimensional dimer rows is not explicitly related to the surface electronic structure. Thus the formation mechanism and the origin of stability of the one-dimensional structures deserve further investigation.

B. Origin of the surface states and the surface reconstruction

Now we turn to the discussion of origins of the surface states S_1-S_4. Unfortunately there is no theoretical calculation on the surface band structures of the 3×2 phase reported to date. This prevents detailed assignments of the surface-state origins. However, the characteristics of the surface-state bands give some important clues about their origins.

Up to now, mainly two different structure models have been discussed for the 3×2 surface: a ''2×3'' model with 1/3 ML of Si ad-dimers on the Si termination layer (the so-called Yan-Semond model) (Refs. 2 and 12) and a ''3×2'' model with $\frac{2}{3}$ ML of Si ad-dimers [the so-called Dayan-Hara model, see Fig. 1(a)].[2,10,11] We recently demonstrated that only the Dayan-Hara model is compatible with our high-resolution core-level photoemission results.[14] Furthermore the Yan-Semond model cannot explain the appearance of the 3×1 phase by hydrogen adsorption and the orientation of the single-domain ''3×2'' LEED pattern,[2,14] which is also confirmed in the present study. In terms of surface electrons, the Dayan-Hara model has four dangling bonds on the Si ad-dimers [solid circles in Fig. 1(a)] and another four dangling bonds on the second layer Si atoms [grey circles in Fig. 1(a)] in a unit cell. We can also count four electrons for the two dimer bonds of the Si ad-dimers and sixteen electrons for the eight back bonds of the Si ad-dimers to the second layer as surface electrons. Basically this electron counting gives an even number of surface electrons in agreement with the semiconducting surface observed: the 3×2 surface has a band gap larger than ~1.2 eV as shown in Figs. 5, 7, and 9.

To a first approximation, one can expect that the most prominent surface electronic states should be due to the eight dangling-bond electrons, which should result in four fully occupied bands. This notion seems to qualitatively agree with the four surface state bands S_1-S_4 found within the bulk band gap: two surface states due to the dangling bonds on the Si ad dimers and the other two due to the dangling bonds on the second layer Si atoms. The dangling-bond surface states are generally expected to have less dispersion than the dimer or back bond surface states, which is consistent with the present results. In addition, the dangling bonds are naturally expected to be the most active sites for adsorption. Thus the clear sensitivity of S_1-S_4 to hydrogen adsorption supports a dangling-bond origin. However, in the same context, one may assign one or two of the four surface states to dimer-bond surface states, since hydrogen adsorption is expected to also break the dimer bonds. This assignment is, however, not so likely since the dimer-bond state is expected to have much larger dispersion than a dangling-bond surface state. It is also worthwhile to note that the dimer-bond surface states have never been clearly observed for Si or Ge dimers on Si(001) (Refs. 32 and 34) and Ge(001) (Ref. 33) surfaces, respectively. The four dangling bonds on the two Si ad-dimers are expected to form two degenerated π bonding states of symmetric dimers, which can split into two levels through an interaction between them. On the other hand, the four dangling bonds on the second layer can induce some bonding between the neighboring second layer Si atoms not bonded to ad-dimers, which leads to a dimerlike reconstruction along [110]. It is not clear whether this reconstruction on the second layer results in π or σ states from the dangling bonds.

The above discussion is, however, based on the assumption that the Si atoms in the additional layer form ''conventional dimers,'' which have the dimer bonds (a σ state) oc-

cupied. However recent *ab initio* calculations of the Si-terminated 3C-SiC(001)2×1 surface showed a very different bond configuration for the Si dimers. That is, the tendency to form a dimer is very weak and the bonding (π) and antibonding (π^*) states of dangling-bond orbitals are fully occupied instead of the dimer bonds (σ).[5,6,38] At present there seems to be no consensus on this weakly bonded dimer configuration since the available experimental study gave a much shorter dimer length than theoretically expected.[39] It is also not clear whether the Si ad-dimers above the Si termination layer have a similar weak tendency of dimerization or not.[40]

If we adopt the idea of ''weak dimerization'' for Si ad-dimers of the 3×2 surface, we expect four fully occupied dangling bond surface states already from Si ad-dimers: two π and two π^* states. Thus one may assign the four surface states observed to these π and π^* states localized on the Si ad-dimers. In this case the topmost surface state should have a π^* symmetry.[6,21] This is definitely inconsistent with the present finding of even symmetries of the topmost surface state S_1 for both of the two mirror planes. Further, this model does not provide any reason why the surface state bands due to the dangling bonds on the second Si layers are not observed. It is still possible to assign some of the four surface states to the π and π^* states of the Si ad-dimers and the remaining to the dangling bonds of the second layer Si atoms. Then, two missing dangling-bond states may be assumed to be degenerate with other surface states or they are not observed due to overlaps with bulk bands. The former possibility, however, seems not so plausible since S_1-S_4 have definite symmetry properties. The latter possibility is not likely either since we have found no evidence for other surface states and/or resonances at binding energies less than 9 eV where the Si dangling-bond states are expected. Thus we conclude that the occupation of π^* states of the Si ad-dimers is inconsistent with the present results and the ad-dimers seem to have a relatively strong tendency to form dimers. The dimer formation was very recently treated in a total energy calculation, which suggests a strong dimerization for the Si ad-dimers on the 3×2 surface.[41]

Very recently Käckell *et al.* have identified two surface state bands on a double-domain Si-terminated 2×1 surface prepared in a Si flux. The binding energies of the two surface states are 1.0 and 3.2 eV as determined by ARPES measurements along the [010] azimuth.[21] These two surface states are similar to S_1 and S_3 in binding energies and peak shapes. Through comparison to theoretically calculated surface band dispersions, they assigned these two bands to π and π^* states of anomalous weakly bonded Si dimers. However, the binding energies and dispersions of these two bands are not in quantitative agreement with their own theoretical calculation.[21] The similarity between S_1 and the topmost surface state reported by Käckell *et al.* makes it very tempting to assign the same origin for these two states. This connection was already discussed in the previous angle-integrated study.[2,19] However we have shown that S_1 has no π^* character in contradiction to the conclusion on the topmost surface state by Käckell *et al.* Thus we think that a further study of the orbital characters and symmetry properties of the surface state bands of the 2×1 surface is needed to make the π (π^*) assignment of Käckell *et al.* decisive and to support their conclusion on the ''weak dimerization.'' It should also be noted that the topmost surface state of the 2×1 surface can be due to the reminiscence of S_1 of the Si ad-dimers, which is not intrinsic to the 2×1 surface. This possibility comes from the facts that the topmost surface state of the 2×1 surface appears at almost the same binding energy as S_1 but with much less intensity [see Fig. 10(a) and Refs. 2 and 19] and that the 2×1 surface prepared in a Si flux can have excessive Si atoms in the form of ad-dimers.

At this time no detailed experimental surface band structure study is available for the cubic SiC(001) surfaces other than the present one of the 3×2 phase and the very recent report on the 2×1 surface discussed above.[21] However, a recent normal emission photoemission study has found a surface state on the Si-terminated $c(4\times2)$ surface at a very similar binding energy to S_1. It is of interest to study this similarity further in order to clarify the origin of the topmost surface state of the $c(4\times2)$ phase.[9] The only available surface band structure study of other SiC surfaces to date is the recent work of Johansson, Owman, and Mårtensson[42] on the 6H (4H)-SiC(001)$\sqrt{3}\times\sqrt{3}$ surface. This work identified one surface state above the VBM at a similar binding energy to S_1. The origin of this surface state has not been discussed probably due to uncertainties in the structure and stoichiometry of the $\sqrt{3}\times\sqrt{3}$ surface.[3,43] An interesting point is that this surface state also showed very small dispersion, less than 0.2 eV, which is similar to the present result for S_1.

V. CONCLUSIONS

The electronic structure of a well-ordered single-domain 3C-SiC(001)3×2 surface has been extensively studied by polarization-dependent angle-resolved photoelectron spectroscopy using synchrotron radiation. The Fermi level position at the surface was accurately determined to be located at 2.1 eV above the valence-band maximum by identifying emission from the topmost valence band (b_1). A very distinctive surface Umklapp scattering of b_1 is also observed along the [110] azimuth (the $\times3$ direction). The 3×2 surface was found to be semiconducting with a band gap larger than $\sim$1.2 eV, which is consistent with the electron counting in the proposed structure model.

Four different surface state bands S_1, S_2, S_3, and S_4 were identified clearly within the bulk band gap at binding energies of 1.4 ± 0.1, 2.3 ± 0.1, 2.9 ± 0.1, and 3.8 ± 0.1 eV, respectively. The topmost surface state S_1 is consistent with the surface state V_1 previously reported by angle-integrated photoemission.[2,19] The surface nature of S_1-S_4 was further confirmed by the photon energy independence of their dispersions. In addition these states are all absent on the 3×1 phase formed by hydrogen adsorption and on the 2×1 and $c(2\times2)$ phases formed by Si sublimation. The two-dimensional band structures of these bands were determined throughout the 3×2 surface Brillouin zone, indicating only very small or no dispersions. These unusually small dispersions suggest a strong electron localization within a unit cell, which is consistent with the recent observation of a cellular disorder for the 3×2 phase.[15] However, the present finding of nondispersing bands without significant anisotropy indicates that there is no strong one-dimensional interaction on the 3×2 surface in contrast to the recent observation of the

formation of very long, highly stable, dimer rows.

Symmetry properties of these surface state bands have been determined using the linear polarization of the incident synchrotron radiation: $S_1(S_3)$ is even (odd) for both mirror planes and S_2 is even and odd for the mirror planes containing the [110] and [1$\bar{1}$0] azimuth, respectively. The symmetry of S_4 is clear only in the plane containing the [1$\bar{1}$0] azimuth, where it has an even symmetry.

From their small dispersions, their energy positions within the bulk band gap and the sensitivity to hydrogen adsorption, we can make a plausible assignment of the S_1-S_4 states as due to dangling bonds of the Si ad-dimers and of the Si second layer within the 3×2 surface reconstruction with 2/3 ML of Si ad-dimers. The symmetry properties of the surface bands observed seem inconsistent with the occupation of π^* states of Si ad-dimers, which rules out the idea of anomalously weak dimerization in the additional Si layer. Further theoretical studies are highly desirable to clarify the origin of these surface states and the bonding configuration of the surface Si dimers on the SiC(001) surfaces.

ACKNOWLEDGMENTS

The authors are grateful to Dr. S. Wiklund for his technical support in Maxlab. H.W.Y. gratefully acknowledges the hospitality of the Maxlab staff, financial support from IFM, Linköping University, and from Professor T. Ohta.

*Author to whom correspondence should be addressed. FAX:+81-298-64-3584. Electronic address: yeom@chem.s.u-tokyo.ac.jp

[1] For example, C. E. Weitzel *et al.*, IEEE Trans. Electron Devices **43**, 1732 (1996).

[2] As a review, see V. M. Bermudez, Phys. Status Solidi B **202**, 407 (1997).

[3] As reviews, see U. Starke, Phys. Status Solidi B **202**, 425 (1997); P. Mårtensson, F. Owman, and L. I. Johansson, *ibid.* **202**, 501 (1997).

[4] J. P. Long, V. M. Bermudez, and D. E. Ramaker, Phys. Rev. Lett. **76**, 991 (1996).

[5] A. Catellani, G. Galli, and F. Gygi, Phys. Rev. Lett. **77**, 5090 (1996).

[6] M. Sabisch, P. Kruger, A. Mazur, M. Rohlfing, and J. Pollmann, Phys. Rev. B **53**, 13 121 (1996).

[7] M. L. Shek, Surf. Sci. **349**, 317 (1996).

[8] P. Soukiassian, F. Semond, L. Douillard, A. Mayne, G. Dujardin, L. Pizzagalli, and C. Joachim, Phys. Rev. Lett. **78**, 907 (1997).

[9] V. Yu. Aristov, L. Douillard, O. Fauchoux, and P. Soukiassian, Phys. Rev. Lett. **79**, 3700 (1997).

[10] M. Dayan, J. Vac. Sci. Technol. A **4**, 38 (1986).

[11] S. Hara, S. Misawa, S. Yoshida, and Y. Aoyagi, Phys. Rev. B **50**, 4548 (1994).

[12] F. Semond, P. Soukiassian, A. Mayne, G. Dujardin, L. Douillard, and C. Jaussaud, Phys. Rev. Lett. **77**, 2013 (1996).

[13] P. Soukiassian, F. Semond, A. Mayne, and G. Dujardin, Phys. Rev. Lett. **79**, 2498 (1997).

[14] H. W. Yeom, Y.-C. Chao, S. Terada, S. Hara, S. Yoshida, and R. I. G. Uhrberg, Phys. Rev. B **56**, R15 525 (1997).

[15] S. Hara, J. Kitamura, H. Okushi, S. Misawa, S. Yoshida, H. W. Yeom, and R. I. G. Uhrberg, Phys. Rev. Lett. (to be published).

[16] V. M. Bermudez, J. Appl. Phys. **66**, 6084 (1989).

[17] T. M. Parrill and Y. W. Chung, Surf. Sci. **243**, 96 (1991).

[18] M. L. Shek, K. E. Miyano, Q.-Y. Dong, T. A. Callcott, and D. L. Ederer, J. Vac. Sci. Technol. A **12**, 1079 (1994). This paper mentioned the 3×2 phase by mistake, which was actually a 2×1 surface as corrected later (see Ref. 7).

[19] V. M. Bermudez and J. P. Long, Appl. Phys. Lett. **66**, 475 (1995).

[20] S. Semond, P. Soukiassian, P. S. Mangat, Z. Hurych, L. di Cioccio, and C. Jaussaud, Appl. Surf. Sci. **104/105**, 79 (1996); F. Semond, L. Douillard, P. Soukiassian, D. Duham, F. Amy, and S. Rivillon, Appl. Phys. Lett. **68**, 2144 (1996).

[21] P. Käckell, F. Bechstedt, H. Hüsken, B. Schröter, and W. Richter, Surf. Sci. Lett. **391**, L1183 (1997).

[22] B. N. Jensen, S. M. Butorin, T. Kaurila, R. Nyholm, and L. I. Johansson, Nucl. Instrum. Methods Phys. Res. A **394**, 243 (1997).

[23] P. Butcher and R. Uhrberg, Phys. World **8** (9), 48 (1995).

[24] H. W. Yeom, Y.-C. Chao, I. Matsuda, S. Hara, S. Yoshida, and R. I. G. Uhrberg (unpublished).

[25] For example, H. W. Yeom, T. Abukawa, Y. Takakuwa, Y. Mori, T. Shimatani, A. Kakizaki, and S. Kono, Phys. Rev. B **53**, 1948 (1996); H. W. Yeom, T. Abukawa, Y. Takakuwa, Y. Mori, T. Shimatani, A. Kakizaki, and S. Kono, *ibid.* **55**, 15 669 (1997).

[26] Y. Li and P. J. Lin-Chung, Phys. Rev. B **36**, 1130 (1987).

[27] H. W. Yeom, I. Matsuda, K. Tono, S. Hara, S. Yoshida, and T. Ohta (unpublished).

[28] K. Sasaki *et al.*, Appl. Phys. Lett. **45**, 72 (1984); S. Yoshida *et al.*, Appl. Phys. Lett. **46**, 766 (1985).

[29] L. S. O. Johansson, R. I. G. Uhrberg and G. V. Hansson, Phys. Rev. B **38**, 13 490 (1988); R. I. G. Uhrberg and G. V. Hansson, Crit. Rev. Solid State Mater. Sci. **17**, 133 (1991).

[30] For example, G. Lévêque, M. Banouni, C. Jouanin, D. Bertho, and J. Bonnet, J. Vac. Sci. Technol. A **11**, 529 (1993).

[31] H. W. Yeom, Y.-C. Chao, S. Terada, S. Hara, S. Yoshida, and R. I. G. Uhrberg (unpublished).

[32] Y. Enta, S. Suzuki, and S. Kono, Phys. Rev. Lett. **65**, 2704 (1990); L. S. O. Johansson, R. I. G. Uhrberg, P. Mårtensson, and G. V. Hansson, Phys. Rev. B **42**, 1305 (1990); P. Krüger and J. Pollmann, Phys. Rev. B **38**, 10 578 (1988).

[33] E. Landemark, C. J. Karlsson, L. S. O. Johansson, and R. I. G. Uhrberg, Phys. Rev. B **49**, 16 523 (1994); E. Landemark, R. I. G. Uhrberg, P. Krüger, and J. Pollmann, Surf. Sci. Lett. **236**, L359 (1990).

[34] K. Tono, H. W. Yeom, I. Matsuda, and T. Ohta (unpublished).

[35] M. C. Håkansson, L. S. O. Johansson, C. B. M. Andersson, U. O. Karlsson, L. Ö. Olsson, J. Kanski, L. Ilver, and P. O. Nilsson, Surf. Sci. **374**, 73 (1997).

[36] P. K. Larsen, J. F. van der Veen, A. Mazur, J. Pollmann, J. H. Neave, and B. A. Joyce, Phys. Rev. B **26**, 3222 (1982); P. K. Larsen and J. F. van der Veen, J. Phys. C **15**, L431 (1982).

[37] W. R. A. Huff, M. Shimomura, N. Sanada, G. Kaneda, T. Takeuchi, Y. Suzuki, H. W. Yeom, T. Abukawa, S. Kono, and Y. Fukuda, Phys. Rev. B **57**, 10 132 (1998).

[38] A. Castellani, G. Galli, F. Gygi, and F. Pellacini, Phys. Rev. B **57**, 12 255 (1998).

[39] J. M. Powers, A. Wander, M. A. van Hove, and G. A. Somorjai, Surf. Sci. Lett. **260**, L7 (1992).

[40] While Sabisch *et al.* addressed that the tendency of very weak dimerization is also present for the Si ad-dimers of the additional

Si layer on the Si termination layer (see Ref. 6), Käckell *et al.* have pointed out the dimerization is stronger for the additional Si layer (see Ref. 21).
[41] P. Käckell (private communication).
[42] L. I. Johansson, F. Owman, and P. Mårtensson, Surf. Sci. **360**, L478 (1996).
[43] L. I. Johansson, F. Owman, and P. Mårtensson, Phys. Rev. B **53**, 13 793 (1996).